Fluorescence Properties of Acrylodan-Labeled Tropomyosin and Tropomyosin–Actin: Evidence for Myosin Subfragment 1 Induced Changes in Geometry between Tropomyosin and Actin†

Sherwin S. Lehrer* and Yoshiharu Ishii

Department of Muscle Research, Boston Biomedical Research Institute, 20 Staniford Street, Boston, Massachusetts 02114, and Department of Neurology, Harvard Medical School, Boston, Massachusetts 02115

Received February 10, 1988; Revised Manuscript Received April 11, 1988

ABSTRACT: The Cys groups of rabbit skeletal tropomyosin (Tm) and rabbit skeletal $\alpha\alpha$Tm were specifically labeled with acrylodan (AC). The probe on Tm is quite immobile yet exposed to solvent as indicated by its limiting polarization (P_0 = 0.38) and fluorescence emission spectrum (λ_{max} = 520 nm) and its accessibility to solute quenching. Changes in the shape of the excitation spectrum with temperature correlated with the helix thermal pretransition and main transition without much spectral change of the emission spectrum. The probe environment of ACTm did not significantly change on binding to F-actin, but fluorescence energy transfer between tryptophan in actin and AC on Tm was indicated by a 15–20% increase in AC fluorescence and a few percent decrease in tryptophan fluorescence. This energy transfer increased when myosin subfragment 1 (S1) was bound to the ACTm–actin filament, in quantitative agreement with the postulated shift in state of Tm associated with the cooperative binding of S1 to actin (Hill et al., 1980). The increase in energy transfer shows that there is a change in the spatial relationship between Tm and actin associated with the S1-induced change in state of Tm.

Tropomyosin (Tm)[1] is an essential component in the Ca-dependent muscle thin filament regulation of muscle contraction (Ebashi & Endo, 1968; Smillie, 1979; Leavis & Gergely, 1984). It is a two-chain coiled-coil α-helical molecule predominantly consisting of a mixture of $\alpha\alpha$ and $\alpha\beta$ molecules in which the α and β chains which differ slightly in amino acid sequence (Mak et al., 1979) are arranged in parallel and in register (Johnson & Smillie, 1975; Stewart, 1975; Lehrer, 1975). An important aspect of regulation is the cooperativity that Tm imparts to the thin filament initially indicated by ATPase studies (Bremel et al., 1972). Thus, although myosin subfragment 1 (S1) binds hyperbolically to the pure or unregulated actin filament, when troponin and Tm are bound to actin (to reconstitute Ca^{2+}-regulated actin) S1 binding becomes sigmoidal (Greene & Eisenberg, 1980). Cooperative S1 binding behavior is also observed when Tm alone is bound to actin (Williams & Greene, 1983) and is also indicated by the S1 dependence of the Tm–acto–S1 ATPase activity (Lehrer & Morris, 1982; Nagashima & Asakura, 1982). This cooperativity was analyzed in terms of a binding model of S1 to the thin filament in which there are two thin filament states—state 1 (for which S1 binding is weak) and state 2 (for which S1 binding is strong) (Hill et al., 1980). Although Tm is predominantly in state 1 in the absence of S1, as S1 binds, Tm is cooperatively shifted to state 2. This model was extended and applied to the kinetics of the ATPase reaction (Hill et al., 1981; Lehrer & Morris, 1982; Hill, 1983).

Recently, we have shown that the S1-induced monomer fluorescence change of pyrene-Tm is a direct measure of the fraction of Tm units in state 2, in agreement with the Hill et al. theory (1980) (Ishii & Lehrer, 1987). To ensure that the results are not probe dependent, we decided to study the properties of acrylodan-labeled Tm. Acrylodan (AC) has the environmental sensitivity of its parent prodan fluorophore (Weber & Farris, 1979) and is specific for Cys groups (Prendergast et al., 1983). In this study, we verified the specificity of the reactivity of AC toward SH groups under denaturing conditions where all side chains are exposed and show that the fluorescence properties of the probe on Tm correlate with Tm's conformational properties. We also show that there is fluorescence energy transfer between actin's tryptophan(s) and the AC group on Tm, which increases as a result of the S1-induced change in the state of Tm.

These data verify that different probes located at Cys-190 on Tm are sensitive to the S1-induced change in the state of Tm. They also indicate that there is a changed distance and/or orientation between certain tryptophan residues in actin and the AC probe on Tm, thus providing evidence for movement of Tm associated with the cooperative binding of S1.

Materials and Methods

Preparation and Labeling of Proteins. Tropomyosin (Tm), actin, and myosin were purified from rabbit skeletal muscle, and their concentrations were determined spectrophotometrically as outlined previously (Morris & Lehrer, 1982). Rabbit skeletal myosin subfragment 1 (S1) was prepared by chymotryptic cleavage of myosin (Weeds & Pope, 1977) using Mg^{2+} to selectively precipitate rod and undigested myosin (Okamoto & Sekine, 1985). To isolate $\alpha\alpha$Tm, rabbit skeletal Tm, a mixture of $\alpha\alpha$ and $\alpha\beta$ molecules, was treated with Nbs_2 [5,5′-dithiobis(2-nitrobenzoate)] which produces α–αTm (disulfide-cross-linked at Cys-190) and Nbsβ–αTm (disulfide-cross-linked at Cys-190 and blocked at Cys-36 with

† Supported by grants from the National Institutes of Health (HL-22461), the National Science Foundation (DMB-8417368), and the Muscular Dystrophy Association. A preliminary report has been presented (Ishii & Lehrer, 1988).

* Address correspondence to this author at the Department of Muscle Research, Boston Biomedical Research Institute.

[1] Abbreviations: AC, acrylodan [6-acryloyl-2-(dimethylamino)-naphthalene]; Tm, tropomyosin; S1, myosin subfragment 1; Hepes, 4-(2-hydroxyethyl)-1-piperazineethanesulfonic acid; Nbs_2, 5,5′-dithiobis-(2-nitrobenzoate); Tempol, 4-hydroxy-2,2,6,6-tetramethylpiperidine-1-oxyl.

0006-2960/88/0427-5899$01.50/0

an Nbs group) (Lehrer, 1975). After dialysis, the two components were separated on an 2 cm × 25 cm column containing hydroxyapatite (Eisenberg & Kielley, 1974) (DNA-grade HTP, Bio-Rad) using 100 mg of protein dialyzed vs starting buffer (20 mM sodium phosphate buffer, pH 7.2) and a 1-L phosphate gradient ending with 0.25 M sodium phosphate buffer (pH 7.2), both solutions containing 1 mM EDTA and 0.5 M NaCl. Some α–αTm was saved for a labeling control, and the remaining α–αTm was reduced with 10 mM dithiothreitol and dialyzed to make $\alpha\alpha$Tm just prior to labeling.

Tm, $\alpha\alpha$Tm, and α–αTm were typically reacted at 7–20 μM in 4 M GdmCl, 10 mM sodium phosphate or Hepes buffer, pH 7.0–7.5, and 1 mM EDTA for 2–4 h at room temperature with 3–6× molar excess acrylodan [6-acryloyl-2-(dimethylamino)naphthalene, Molecular Probes] by adding microliter quantities of a stock solution dissolved in dimethylformamide. The solutions were quenched with 5 mM dithiothreitol and dialyzed to renature and remove unreacted reagents. The labeling ratio varied from 1.3 to 1.7 AC/Tm using ϵ_{365}(AC) = 12900 M^{-1} cm^{-1} (Prendergast et al., 1983) and [ACTm] determined by the BCA–protein assay (Pierce) using unlabeled Tm as a standard with E_{277} = 0.24 $(mg/mL)^{-1}$ cm^{-1} (Lehrer, 1975). Lightly labeled AC$\alpha\alpha$Tm was prepared by mixing 0.09 mg of AC$\alpha\alpha$Tm (labeling degree = 1.4 AC/Tm) with 0.44 mg of unlabeled $\alpha\alpha$Tm in 4 M GdmCl, 10 mM dithiothreitol, 10 mM sodium phosphate buffer, pH 7.0, and 1 mM EDTA (which separated the chains) and dialyzed vs buffer in the absence of GdmCl and dithiothreitol (to renature the chains), resulting in 0.23 AC/Tm.

β-Mercaptoethanol (20 μM) was labeled by reacting with AC (10 μM) at pH 7 and monitored fluorometrically until completed. To ensure that all AC was reacted, a few micromolar β-mercaptoethanol was added. Dilutions were made into appropriate solvents for study.

Optical Measurements. Lifetime measurements were performed and analyzed by Dr. Gerrard Marriott in the Biochemistry Department, University of Illinois, Champaign—Urbana, with a multifrequency phase fluorometer and associated software programs (Alcala et al., 1987). The $\alpha\alpha$Tm sample at 4 μM in 10 mM sodium phosphate buffer, pH 7.0, 0.5 M NaCl, and 1 mM EDTA was excited at 325 nm with a He–Cd laser, and the emission was filtered through a Corning 0-52 glass filter which effectively collected the entire emission.

Steady-state fluorescence spectra were obtained with a Spex Fluorolog 2/2/2 photon-counting fluorometer (Edison, NJ) in the ratio mode with either a 2.25- or a 4.5-nm band-pass with a 300-nm blazed grating for excitation and either a 500- or a 300-nm blazed grating for AC or tryptophan emission spectra, respectively. The S1 titrations on ACTm–actin were performed by programming the Datamate computer to cycle between excitation wavelengths (X) and emission wavelengths (M) to indicated values of X/M (in nanometers), in order to measure light scattering (365/374), energy transfer (295/510), and direct excitation (365/510) after each addition of S1 in the same cuvette, to time-average each measurement for 20 s, and to tabulate the data after correction for dilution. The data were then fitted to the equations of Hill et al. (1980) using a nonlinear least-squares fitting program written by Dr. Edward P. Morris.

Polarization data were obtained on the Spex fluorometer with Glan–Thompson prisms in the L format and calculated by using a measured grating correction factor. Solute quenching was performed with the water-soluble nitroxide tempol (4-hydroxy-2,2,6,6-tetramethylpiperidine-1-oxyl, Molecular Probes) by adding microliter quantities of a 0.2 M solution in H_2O, with monochromators set at 335/540 to minimize inner filter effects. Corrections (<30%) were made for absorption of tempol with F(corr) = F(uncorr) × $10^{A/2}$.

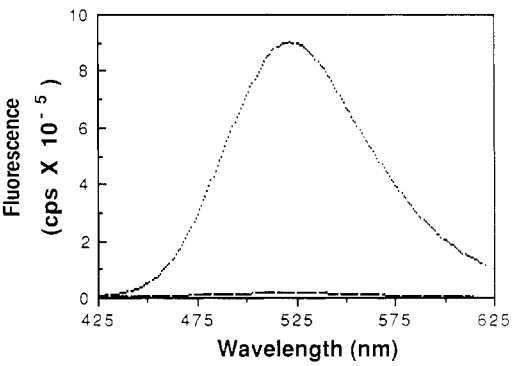

FIGURE 1: Fluorescence emission spectra of AC$\alpha\alpha$Tm (···) and control α–αTm (– –) treated with AC. The Cys groups of α–αTm were blocked by disulfide cross-linking with Nbs_2 prior to AC reaction. λ_{exc} = 365 nm, 24 °C, [AC$\alpha\alpha$Tm] = [α–αTm] = 7 μM in 0.5 M NaCl, 10 mM sodium phosphate buffer, pH 7.0, and 1 mM EDTA.

Circular dichroism data were obtained with an Aviv Associates 60DS instrument (Lakewood, NJ) whose computer controlled the heating rate (0.4 °C/min) of a Hewlett Packard thermoelectric temperature controller. The temperature was monitored with a probe in contact with the stirred solution, and the ellipticity was recorded after 0.5-min equilibration time and 10-s data averaging after each step of 0.2 °C. Absorption spectra were obtained with either a Perkin-Elmer λ 3 or a Beckman DU-40 spectrophotometer.

RESULTS

Fluorescence Properties of ACTm. Acrylodan (AC) reacts specifically with the Cys groups of $\alpha\alpha$Tm. This was shown by a comparison of the kinetics and extent of reaction with two samples, one having free SH groups (no disulfide cross-links, represented as $\alpha\alpha$Tm) and a control sample which had its interchain Cys-190 groups disulfide-cross-linked by prior reaction with Nbs_2 (represented as α–αTm). Both samples were identically treated with AC in the denatured state and renatured as outlined under Materials and Methods. At a 3× molar ratio of AC to SH groups, the covalent attachment with $\alpha\alpha$Tm took about 4 h with a half-life of 40 min and resulted in a fluorescence enhancement of about 10×. In contrast, α–αTm treated with AC did not show any fluorescence change when monitored for 2 h. The fluorescence spectra which were measured after removal of quenched unreacted reagent and renaturation showed a lack of appreciable fluorescence exhibited by the α–αTm control sample (Figure 1). Three different AC-labeled Tm's were studied: (i) AC$\alpha\alpha$Tm with a low degree of labeling where most labeled molecules contain only one AC/Tm; (ii) AC$\alpha\alpha$Tm with a high degree of labeling where most labeled molecules contain two AC/Tm; (iii) AC rabbit skeletal (RS) Tm (ACRSTm, a mixture of AC$\alpha\alpha$Tm and AC$\alpha\beta$Tm molecules). All ACTm's essentially showed the same emission and excitation spectra. This indicated that (i) two AC moieties at the Cys-190's as opposed to one did not change the AC environment and (ii) AC-labeled $\alpha\alpha$Tm and $\alpha\beta$Tm, the two components of RSTm, have similar AC environments at Cys. In discussing results that have been shown to be valid for all of the above samples, the term ACTm will therefore be used.

The location of the fluorescence peak at 520 nm for ACTm indicates that the probe is located in a polar environment in view of the 100-nm red shift that AC–β-mercaptoethanol

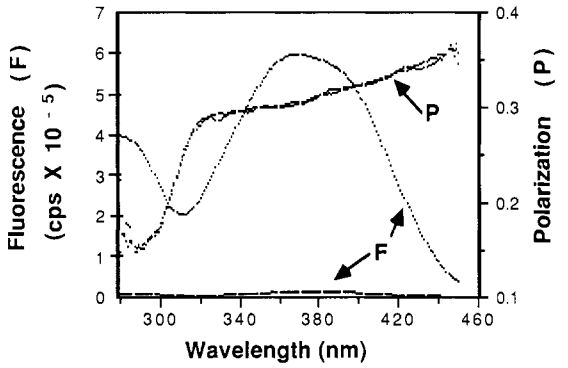

FIGURE 2: Excitation fluorescence (F) and polarization (P) spectra (two determinations) of AC$\alpha\alpha$Tm (···) and fluorescence spectrum of AC-treated α–αTm (– –). λ_{em} = 510 nm. Same sample conditions as Figure 1.

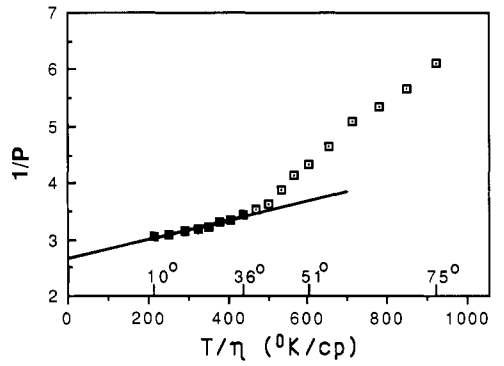

FIGURE 3: Perrin plot of the temperature dependence of polarization of fluorescence of AC$\alpha\alpha$Tm showing points used in a linear extrapolation to limiting polarization (■) and sensitivity to the thermal transition above 40 °C. λ_{exc} = 365 nm, λ_{em} = 510 nm. [AC$\alpha\alpha$Tm] = 1.0 μM in 0.5 M NaCl, 5 mM $MgCl_2$, and 10 mM Hepes buffer, pH 7.5.

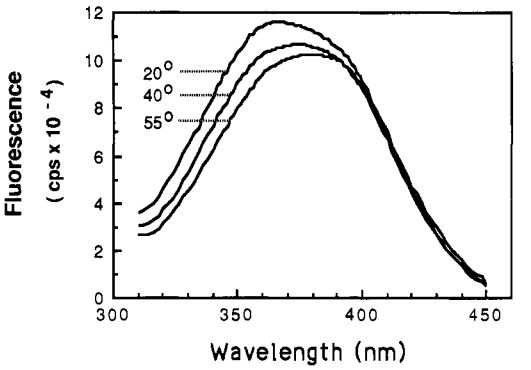

FIGURE 4: Shift of the excitation spectrum of AC-labeled rabbit skeletal Tm with temperature. λ_{em} = 510 nm. [ACTm] = 0.68 μM in 0.5 M NaCl, 1 mM EDTA, and 20 mM Hepes buffer, pH 7.5.

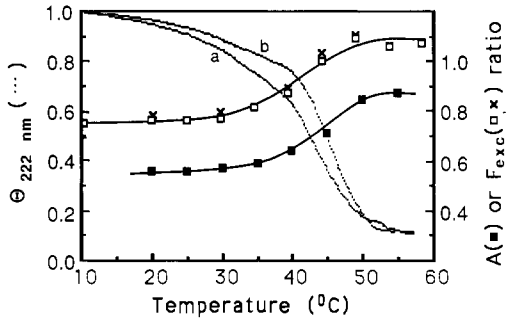

FIGURE 5: Correlation of the temperature dependence of the absorption, and fluorescence excitation spectral changes of AC-labeled rabbit skeletal Tm with its thermal helix unfolding transitions. A ratio (A_{415nm}/A_{335nm}) (■), [ACTm] = 2.3 μM; F_{exc} ratio (F_{415nm}/F_{335nm}) at increasing T (□) and decreasing T (×), λ_{em} = 510 nm, [ACTm] = 0.68 μM; θ_{222nm}, normalized ellipticity of α-helix, (a) [ACTm] at 0.60 μM, (b) [Tm] at 0.76 μM. All samples in 0.5 M NaCl, 1 mM EDTA, and 20 mM Hepes buffer, pH 7.5.

adducts experience in going from dioxane (435 nm) to water (540 nm) (Prendergast et al., 1983). Our finding that the emission maxima of the AC–β-mercaptoethanol adduct were at 535 and 506 nm, in water and ethanol, respectively, with about a 6× greater quantum yield in ethanol supports the previous study. The relative quantum yield of AC$\alpha\alpha$Tm was only about 1.3× that of the AC–β-mercaptoethanol adduct in water, further indicating a polar environment, in view of the 3–4× greater yield shown for the adduct in organic solvents compared to water (Prendergast et al., 1983).

Studies of the fluorescence lifetime as well as the fluorescence excitation polarization spectrum of AC$\alpha\alpha$Tm indicated some heterogeneity of probe fluorescence at 20 °C with satisfactory fits either to the lifetime data using two components with 2.4 (67%) and 1.0 ns (37%) or to a Lorentzian distribution centered at 1.9 ns with a half-width of 0.9 ns. Although the polarization excitation spectrum was qualitatively similar to that of prodan in glycerol/water at 77 K (Weber & Farris, 1979), the polarization values of AC$\alpha\alpha$Tm increased to a greater extent at the red side of the band (Figure 2). This indicates that there are at least two ground-state environments for the probe on Tm differing somewhat in polarity. A small difference in excited-state environment was also indicated by a 2–3-nm red shift in emission on excitation at the red side of the band (at 415 nm). Previous studies of prodan in water also indicated at least two lifetimes of about 1 and 2 ns, interpreted as due to two conformers of prodan interacting differently with the solvent (Marriott, 1987). The more polar component of AC$\alpha\alpha$Tm associated with the red-shifted absorption spectrum is expected to have the somewhat shorter lifetime (Weber & Farris, 1979; Macgregor & Weber, 1986). This is consistent with the higher degree of polarization observed assuming a similar degree of probe immobilization. Information about the average rotational mobility of the probe was obtained from a Perrin plot (Figure 3). This showed a large decrease in polarization above 40 °C, in agreement with previous unfolding studies (see below). Extrapolating the plot to $T/\eta = 0$ gave a value of 0.38 for the limiting polarization, P_0. This value is not far from the value for immobilized prodan in glycerol/water at −70 °C (0.43) (Weber & Farris, 1979), indicating a relatively rigid environment for the probe on Tm.

The temperature dependence of the fluorescence and absorption spectra of ACRSTm was compared with its helix loss in view of the previously noted multiple thermal unfolding transitions of Tm (Woods, 1976; Lehrer, 1978; Williams & Swenson, 1981; Potekhin & Privalov, 1982; Betteridge & Lehrer, 1983; Hvidt, 1986). The main observation is that there is a change in shape of the excitation (and absorption) spectrum over the 30–55 °C temperature region, indicating that the ground-state environment of the acrylodan changes with temperature (Figure 4). There was only a slight red shift of the emission spectra over the same temperature range (1–2 nm) with only a 100 cm^{-1} increase in half-width from the 20 °C value of 2900 cm^{-1}. These data indicate that solvent relaxation in the excited state is essentially complete at 10 °C. The shape change was quantified by calculating the 415-nm/335-nm absorption and fluorescence excitation ratio. The temperature dependence of these ratios indicated transitions that closely paralleled the transitions in the helix unfolding profile measured with circular dichroism (Figure 5), indicating that the AC environment is affected both by the helix pretransition (25–40 °C) and by the main transition (40–60 °C).

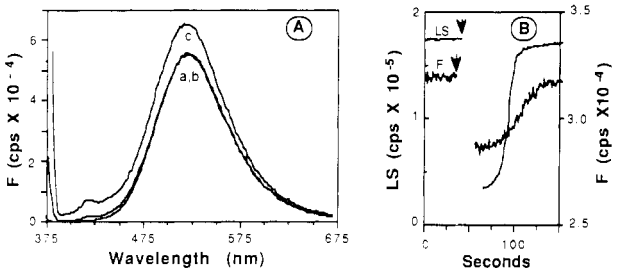

FIGURE 6: Fluorescence effects of the binding of lightly labeled AC$\alpha\alpha$Tm to F-actin and the binding of myosin subfragment 1 to the F-actin–AC$\alpha\alpha$Tm complex. (A) Emission spectra: (a) AC$\alpha\alpha$Tm; (b) AC$\alpha\alpha$Tm + F-actin; (c) AC$\alpha\alpha$Tm + F-actin + S1. [AC$\alpha\alpha$Tm] = 1.0 μM with [AC]/[Tm] (labeling degree) = 0.23, [actin] = 6.5 μM, [S1] = 8.2 μM, in 0.03 M NaCl, 5 mM $MgCl_2$, and 10 mM Hepes buffer, pH 7.5, 25 °C, λ_{exc} = 365 nm. (B) Effect of ATP addition (0.5 mM at arrow) on the fluorescence (F) at 512 nm and light scattering (LS) at 374 nm of the S1–actin–AC$\alpha\alpha$Tm complex of curve c in (A). Note the reversal of F and LS after the ATP was hydrolyzed by the actomyosin ATPase.

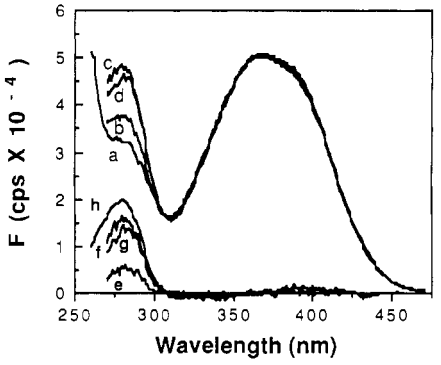

FIGURE 7: Excitation spectra of AC-labeled rabbit skeletal Tm in complexes with F-actin and F-actin and myosin subfragment 1 (S1): (curve a) ACTm alone; (curve b) ACTm + F-actin; (curve c) ACTm + F-actin + S1, [S1]/[actin] = 2/7; (curve d) ACTm + F-actin + S1, [S1]/[actin] = 7/7; (curve e) curve b – curve a; (curve f) curve c – curve a; (curve g) curve d – curve a; (curve h) tryptophan excitation spectrum of F-actin. [F-Actin] = 2.8 μM, [ACTm] = 0.4 μM in 0.03 M NaCl, 5 mM $MgCl_2$, and 20 mM Hepes buffer, pH 7.5, λ_{em} = 510 nm, 25 °C. For curves a–d, spectra obtained from the same systems with unlabeled Tm were subtracted to correct for any possible small contribution of directly excited tryptophan fluorescence. Curves c and d were normalized at 365 nm to correct for directly excited acrylodan.

A slight perturbation by the label was noted by a small shift of the main transition to lower temperature and an increase in the magnitude of the pretransition. A similar perturbation by dansylcystine at Cys-190 had been previously observed (Betteridge & Lehrer, 1983). The perturbation by pyrenylmaleimide at Cys-190 was somewhat greater than AC since in addition to the above-noted perturbations, the initial helix content was also reduced (Ishii & Lehrer, 1985). Similar fluorescence results were obtained for a sample of AC$\alpha\alpha$Tm (data not shown).

Interaction of ACTm with Actin. Although separate binding studies indicated that almost all of the AC$\alpha\alpha$Tm was bound to actin, the emission spectrum of AC$\alpha\alpha$Tm (and ACRSTm) did not change on addition of F-actin (Figure 6A). Spectroscopic evidence for binding was obtained by monitoring changes in excitation spectra associated with AC emission. In the absence of actin, the excitation spectrum of ACRSTm consisted of a main band at 365 nm and a small shoulder in the 275–300-nm spectral region (Figure 7, curve a). This shoulder was also observed in absorption and excitation spectra of AC adducts of β-mercaptoethanol and dithiothreitol, indicating that it is due to direct excitation of AC. In the

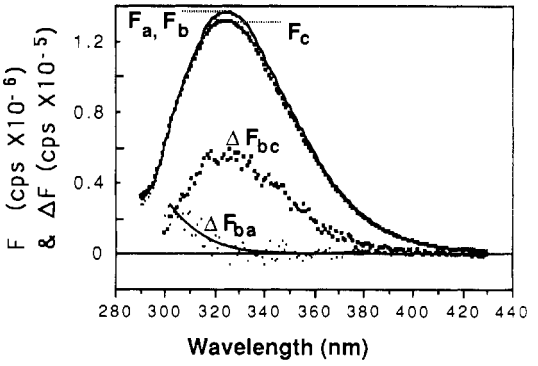

FIGURE 8: Tryptophan emission spectra of actin in the absence and presence of AC-labeled rabbit skeletal Tm and control unlabeled Tm. F_a, actin alone; F_b, actin + unlabeled Tm; F_c, actin + ACTm; $\Delta F_{bc} = 10(F_b - F_c)$; $\Delta F_{ba} = 10(F_b - F_a)$. Conditions as for Figure 7.

presence of actin, a distinct peak at 280 nm was produced (Figure 7, curve b). The actin-induced difference spectrum (curve e) looks very similar to the tryptophan excitation spectrum of actin (curve h), showing that energy transfer from tryptophan of actin to AC on Tm occurs. Although the tryptophan sensitization increased the AC fluorescence by about 15–20%, the actual tryptophan energy transfer only amounted to a few percent. The spectrum of the quenched tryptophan fluorescence in the presence of ACRSTm was measurable compared with the lack of change of actin fluorescence in the presence of unlabeled Tm (Figure 8). Note that the ACRSTm-induced difference spectrum, ΔF_{bc}, which is 10× amplified, has the same spectrum as F-actin, indicating that the tryptophan(s) that contribute(s) to the energy transfer is (are) located in the same environment as the tryptophans that contribute to the overall fluorescence.

Effects of S1 Binding to the ACTm–Actin Complex. Binding of S1 to the actin–ACTm complex produced a 20% increase and a 2-nm blue shift in ACTm fluorescence (Figure 6A), indicating a small environmental change. The binding also produced a large increase in 90° light scattering, which allowed for a convenient method to monitor both the direct binding of S1 and the effects on the fluorescence of ACTm bound to actin. Addition of ATP, which dissociates S1 from actin, reversed the fluorescence and light-scattering changes which eventually recovered after all of the ATP was hydrolyzed by the acto–S1 ATPase (Figure 6B).

Solute quenching studies were performed to determine if the S1-induced slight blue shift was associated with decreased solvent accessibility of the AC moiety. Iodide was not used because it depolymerizes actin, and acrylamide could not be used because it did not quench prodan fluorescence. Tempol, which is a water-soluble nitroxide with an unpaired electron, was an efficient quencher of prodan with linear Stern–Volmer plots giving K_Q = 11.8 M^{-1}. With τ = 2.25 ns (Weber & Farris, 1979), $k_q = 5.2 \times 10^9$ M^{-1} s^{-1}. Linear Stern–Volmer plots were also obtained for tempol quenching of AC$\alpha\alpha$Tm–actin with $K_Q = 6.5 \pm 0.5$ M^{-1} in both the absence and presence of S1, which gives $k_q = 3.4 \times 10^9$ M^{-1} s^{-1} if the average value of τ = 1.9 ns is used. Thus, the AC probe in the Tm–actin complex is quite accessible and does not appreciably change on binding S1, despite the 2-nm blue shift.

An additional effect of S1 binding to ACTm–actin was observed which indicated a change in the relative distance between, and/or relative orientation of, AC on Tm and tryptophan in actin. Excitation spectra showed that the tryptophan–AC energy transfer was increased by the binding of two S1's per seven actin subunits to the ACRSTm–actin complex (Figure 7, curves c and f). Further additions of S1

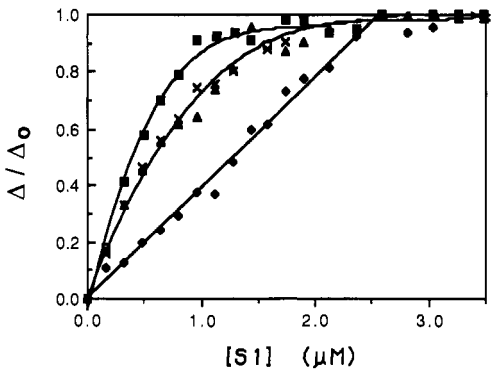

FIGURE 9: Fluorescence and light-scattering changes associated with the binding of myosin subfragment 1 to AC-labeled rabbit skeletal Tm–F-actin complex. LS (♦), light scattering at 374 nm; F_{365} (▲), fluorescence excited at 365 nm; F_{295}/F_{365} (■), energy transfer from tryptophan to acrylodan; (×) points calculated with (×) = 0.7(■) + 0.3(♦). [Actin] = 2.5 μM, [ACTm] = 0.4 μM. λ_{em} = 510 nm. Solution conditions as for Figure 7.

did not increase tryptophan-sensitized AC fluorescence when monitored at 290 nm and above (curves d and g). The decrease in fluorescence below 290 nm at the greater concentration of S1 is due to inner filter effects caused by the absorbance of S1. It should be pointed out that the excitation curves in the presence of S1 in Figure 7, curves c and d, were normalized at 365 nm in order to correct for the increase in the directly excited AC fluorescence noted above. This correction assumes that the fractional increase in directly excited AC fluorescence is the same at 295 nm as at 365 nm, an assumption borne out by the similarity of the S1-induced difference spectra obtained after normalization (Figure 7, curves f and g) to the excitation spectrum of actin's tryptophan fluorescence (Figure 7, curve h), with little or no contribution above about 310 nm. The possibility that the increased tryptophan energy transfer came from the tryptophans of bound S1 rather than from actin was ruled out by S1 titrations.

S1 titrations were performed by monitoring three optical parameters after additions of S1 to ACTm–actin; (i) the light scattering, a direct measure of S1 binding; (ii) the AC fluorescence directly excited at 365 nm, a measure of the S1-induced environmental change of AC; (iii) the AC fluorescence excited at 295 nm, a measure of the S1-induced tryptophan-sensitized AC fluorescence. The actual tryptophan-sensitized AC fluorescence was obtained by correcting for effects of direct excitation of AC at 295 nm by calculating the 295-nm/365-nm fluorescence ratio. The data show that the energy transfer rises sharply and saturates at low ratios of bound S1 (Figure 9). This indicates that the increased energy transfer does not correlate with the observed linear stoichiometric binding of S1 to actin (from the increased light scattering) and therefore rules out energy transfer from S1's tryptophans. The possibility that the increase in energy transfer is simply the result of S1-induced binding of the small fraction of ACTm that was not bound to actin under these conditions (Eaton, 1976) is also ruled out because the three different samples of ACTm with different degrees of labeling showed similar titration profiles and fluorescence enhancements despite affects of labeling degree on actin binding (Ishii & Lehrer, 1985), which would lead to different amounts of unbound ACTm. The corrected energy transfer (295-nm/365-nm fluorescence ratio) therefore reflects the S1-induced change in state of Tm independent of an S1-induced environmental change of AC on Tm.

The titration profile which monitors the environmental change of AC (fluorescence excited at 365 nm, Figure 9) does not rise as sharply as the energy-transfer profile. This can be explained by the combination of two effects contributing to the environmental change of AC: (i) an S1-induced change in state of Tm which affects the AC environment; (ii) a direct effect of S1 binding to an actin subunit near the AC label on Tm. The latter effect should follow the binding profile of S1 to actin while the former effect should follow the S1-induced change in state. A linear combination of the two curves with 70% change in state (from energy transfer) and 30% direct binding of S1 (from light scattering) is seen to fit the experimental data for the 365-nm excitation curve quite well.

Thus, these data indicate that the binding of one to two S1's to actin subunits in a regulatory unit containing one Tm and seven actin molecules causes a change in state in Tm resulting in (i) a changed geometry between the tryptophan of actin and the AC probe on Tm and (ii) an environmental change of the probe. Additional binding of S1 to the actin unit close to the probe on Tm results in an additional environmental change of AC.

Discussion

Fluorescence Properties of ACTm. Acrylodan was developed as a fluorescence labeling reagent (Prendergast et al., 1983) in order to couple the ability to specifically label Cys groups of proteins with the environmental sensitivity of the prodan fluorophore (Weber & Farris, 1979). We have verified the specificity toward Cys groups under conditions in which all groups are equally available for reaction, i.e., GdmCl-denatured Tm. After renaturation of labeled Tm, we found that the acrylodan-labeled Cys-190 groups are quite exposed to the aqueous solvent from the position of the fluorescence spectrum and from studies of solute quenching. The location of the emission peak at 520 nm indicates that it may be the most exposed of any SH-labeled protein thus far studied (Prendergast et al., 1983). Despite its exposure, polarization of fluorescence studies have indicated that it is relatively immobile. These properties are consistent with the expected close packing of the side chains in the coiled-coil α-helical Tm molecule.

The temperature dependence of the steady-state fluorescence of ACTm showed changes that correlated with the known unfolding properties of Tm. Interestingly, although the emission spectrum did not appreciably change with temperature, the fluorescence excitation spectrum shifted to the red. The shift, measured by the ratio of the fluorescence intensities excited at the red vs the blue side of the main band, correlated with the helix unfolding. Thus, the shift was sensitive both to the unfolding pretransition between 30 and 40 °C and to the main transition between 40 and 50 °C. Previous studies with other fluorescence probes at Cys-190 have also shown correlation of fluorescence properties with unfolding properties (Graceffa & Lehrer, 1980; Ishii & Lehrer, 1985; Betteridge & Lehrer, 1983). Although temperature affected the dynamic quenching processes operating on ACTm in the excited state since the emission yield decreased with temperature, the excited-state energetics were not affected by temperature because of the lack of appreciable change in the spectrum. The energetics of the interaction of the probe with its ground-state environment, however, were affected by the unfolding. These observations are understandable in view of the 10× increase in dipole moment upon excitation (Weber & Farris, 1979). In the excited state, the strong interaction of the dipole moment with the polar environment allowed for a more favorable interaction to be obtained even in the folded state, through solvent relaxation. In the ground state, however, the weaker interaction does not allow for such reorientation (Macgregor

& Weber, 1986) until unfolding and solvent exposure take place. Further studies of the temperature and wavelength dependence of the fluorescence lifetimes will clarify the heterogeneous fluorescence at low temperature and the relationship with the unfolding intermediates present.

Interaction of ACTm with Actin. The lack of change of the fluorescence emission spectrum of ACTm on binding to actin suggests that the region around Cys-190 does not interact with actin. Previous studies with pyrenylmaleimide-labeled Tm (Ishii & Lehrer, 1985) and with a nitroxide spin-labeled Tm (Graceffa, 1985) also did not indicate a direct probe–actin interaction, but studies of solute quenching of IAEDANS-labeled Tm showed a small degree of interaction (Lamkin et al., 1983). Analyses of amino acid sequence repeats (McLachlan & Stewart, 1978; Phillips et al., 1986) and of gene structure (Ruiz-Opazo & Nadal-Ginard, 1987) have indicated that there are repeating regions along the rodlike Tm molecule which appear to interact with actin subunits. In all of these studies, Cys-190 is located near a boundary between actin-interacting regions, in agreement with the fluorescence probe studies which showed little or no fluorescence change.

Despite the lack of fluorescence emission change, excitation spectral evidence for ACTm binding to actin was obtained which indicated tryptophan fluorescence energy transfer from actin to AC on Tm (Tm has no tryptophan). It was surprising to be able to observe energy transfer since all but one or two actin subunits would be located too far away from Cys-190 to transfer and each actin contains four tryptophyl residues (Elzinga et al., 1973) or 4 × seven tryptophyls in the one Tm per seven actin subunit complex, TmA_7. In view of the several possible donors, the low degree of transfer, and the lack of characterization of the relative orientation of the donors and acceptor, it is impossible to obtain meaningful distance information. Although the energy transfer amounted to only a few percent, as seen by the decrease in tryptophan fluorescence, the increase in AC fluorescence, or sensitization by tryptophan, was about 5× greater, because of the greater absorbance of tryptophan at 290 nm relative to AC and the fluorescence properties of the tryptophans involved.

Effects of S1 on ACTm–Actin. These studies show that the binding of one to two S1's to the Tm–actin complex, consisting of one Tm interacting with seven actin subunits (TmA_7), increases the energy transfer between actin and Tm. The change in energy transfer cannot be interpreted solely in terms of a distance change if a change in the orientation factor between donor and acceptor transition moments also occurs. The polarization studies indicated that the AC is relatively immobile, and the fluorescence properties of actin indicate the fluorescing tryptophyl residues are mainly buried in hydrophobic environments (Lehrer & Kerwar, 1972) and therefore also probably relatively immobile. Thus, enough rotational motion does not appear to take place to assume that the orientation parameter is the spherically averaged value. The increase in energy transfer can therefore be either due to a decrease in distance between donor and acceptor or due to a change in relative orientation between donor and acceptor without a change in distance, or both. In either case, it can be concluded that there is a change in the geometrical arrangement between the Cys-190 region of Tm and a region in actin containing one or more tryptophans.

The S1 titrations showed that the fluorescence energy transfer increase was half-complete at a binding ratio of about 1 S1/7 actin subunits, similar to the earlier finding with the use of the monomer fluorescence of pyrenylmaleimide-labeled

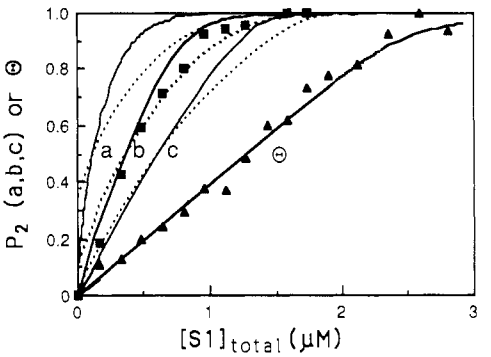

FIGURE 10: Calculated titration curves for different cooperativity parameters under conditions of stoichiometric binding of S1 to Tm–actin. θ is the fraction of actin sites occupied; P_2 is the fraction of Tm units in state 2. The curves were calculated with the equations of Hill et al. (1980) for different cooperativity parameters L' and Y using $K_2 = 5 \times 10^7$ M^{-1}, $K_1 = 0$, and [actin] = 2.5 μM. P_2 curves a, b, and c are for $L' = 2$, 10, and 100, respectively, for two values of Y: 1 (···) and 10 (—). The same θ curve was obtained for all six sets of L' and Y values. The experimental light-scattering data (▲) and fluorescence energy-transfer (■) data of Figure 9 are included.

Tm under similar conditions (Ishii & Lehrer, 1985). In that first report of the S1-induced change in state of Tm, a simple statistical model was considered in which the random binding of S1's to the TmA_7 unit caused the Tm shift (Ishii & Lehrer, 1985). The simple model showed that the cooperative binding of a small number of myosin heads was necessary to change the Tm state. The more complete two-state cooperative binding theory of Hill et al. (1980), which takes into account the weak S1 binding in state 1 and end-to-end interactions, was used to fit the new data. In this cooperative binding model, although Tm predominantly exists in state 1 in the absence of S1, it shifts to state 2, since the affinity of S1 for actin is much greater when Tm is in state 2. The fraction of Tm units in state 2 is given by P_2, and the fraction of actin sites occupied by S1 is given by θ. For illustration, we have plotted P_2 and θ vs total [S1] for three different values of L' (the equilibrium constant for the state 2 to state 1 transition), 2, 10, and 100, for two different values of Y (the end-to-end cooperativity parameter), 1 and 10, at each L' (Figure 10). We used a value of $K_2 = 5 \times 10^7$ M^{-1} for the S1 binding constant when Tm is in state 2, a reasonable value at the low ionic strength used in the above experiments. The curves were not affected if greater values of K_2 were used since essentially all of the S1 added is bound under these conditions. A value of $K_1 = 0$ for the state 1 S1 binding constant was used. The P_2 curves were not appreciably affected as long as the K_1 value was less than about $10^{-2}K_2$ (Hill et al., 1980). It can be seen that, under these stoichiometric binding conditions, whereas the θ vs $[S1]_{total}$ curves are essentially independent of the values of L' and Y, the P_2 curves are quite sensitive to these values. The L' value can readily be obtained from the [S1]/[actin] ratio at $P_2 = 0.5$ since for a given L' value, all of the Y curves pass through this point. Increases in Y result in P_2 curves with increased steepness, seen most clearly for $P_2 > 0.5$. The experimental light-scattering and energy-transfer data of Figure 9 reproduced on the family of curves of Figure 10 show that it is possible to obtain reasonable estimates for L' and Y. Best fits of the data gave values of $L' = 15$ and $Y = 5$ for $K_1 = 0$ or $L' = 10$ and $Y = 5$ for $K_1 = 2.5 \times 10^6$ M^{-1} in both cases using $K_2 = 5 \times 10^7$ M^{-1} (fits not shown). Studies of binding under weaker binding conditions (the presence of nucleotides) which will give better estimates of K_1 (Greene, 1982) will result in better estimates of L'. The above values are in reasonable agreement with cooperativity parameters obtained from pre-

vious studies of Tm–actin considering differences in conditions (Lehrer & Morris, 1982; Williams & Greene, 1983).

The S1-induced AC environmental change, measured by the increase in emission intensity on direct excitation of AC (at 365 nm), was also monitored during S1 titrations. Although the profile was very similar to the energy-transfer profile, it did not rise as sharply at higher [S1]. From curve fitting, it appears that most of the change (about 70%) is due to an environmental change of AC associated with the change in state of Tm (same profile as the energy-transfer change). About 30% of the change, however, appears to be due to an environmental change at AC resulting from the direct binding of S1 to actin near the Cys-190 region of Tm. The environmental change associated with the change in state could either be due to a changed interaction between AC and Tm or be a new interaction between the probe and actin. The direct effect could be due to an interaction between the S1 and the AC probe on Tm. Evidence has been presented for a direct interaction between S1 and Tm from cross-linking studies (Tao & Lamkin, 1984).

Previous studies with the reconstituted Ca^{2+}-sensitive thin filament troponin–Tm–actin, $TnTmA_7$, showed that the monomer fluorescence of pyrene-Tm was also sensitive to the S1-induced change in Tm state (Ishii & Lehrer, 1987). Although we obtained data under similar conditions as the present study, i.e., stoichiometric binding of S1, we did not report L' and Y values from that data because more complete data were obtained in the presence of ADP, and L' and Y are independent of nucleotide (Greene, 1982). Due to effects of some contaminating ATP in the ADP preparations used, however, the cooperativity of the transition for the reconstituted system appears greater than recent studies indicate, which invalidate the cooperativity values previously reported (Figure 2; Ishii & Lehrer, 1987). Values of L' estimated from the limited data in the stoichiometric titrations (Figure 1; Ishii & Lehrer, 1987) give $L' = 2$ and 20, in the presence and absence of Ca^{2+}, respectively. The conclusions of the previous work are still valid: that although Ca^{2+} does not appreciably change the Tm state in the absence of S1, it acts as an allosteric effector to facilitate the S1-induced Tm change in state (Hill et al., 1980). Studies are continuing with AC-labeled systems to obtain better data.

Preliminary studies have indicated that the excimer fluorescence of pyrenyliodoacetamide-labeled Tm also probes the S1-induced change in state, without the problems caused by the slow equilibrium of the excimer fluorescence experienced with the pyrenylmaleimide-labeled Tm system (Ishii & Lehrer, 1985). Other preliminary studies with $\alpha\beta$Tm labeled predominantly at Cys-36 of β with AC showed similar S1-induced changes in state. All of these studies indicate that probes with different properties and located in two different regions of Tm sense the change in state that Tm undergoes in response to the cooperative binding of S1 to the Tm–actin thin filament. They therefore verify the theory of Hill et al. (1980) by providing direct measurements of the Tm change in state which was previously inferred from S1 binding.

In summary, these studies indicate that myosin induces Tm movement on the actin filament. Our earlier studies also indicated that Ca^{2+} probably did not cause Tm movement (Tao et al., 1983). It is difficult to reconcile our results with structural studies which suggest Ca^{2+}-induced Tm movement (Haselgrove, 1972; Huxley, 1972; O'Brien et al., 1975; Kress et al., 1986) but no additional Tm movement associated with myosin crossbridge attachment to the thin filament on muscle activation (Kress et al., 1986). In agreement with the current studies which point to the independence of Tm state on Ca^{2+}, per se, our ATPase studies showed that at very low [S1], Tm largely inhibits acto–S1 activity even in the presence of troponin and Ca^{2+} (Lehrer & Morris, 1982). To take into account the Ca^{2+}-induced movement indicated by structural studies, however, we suggested at that time that Tm state 1 could be subdivided into states 1a and 1b, for $-Ca^{2+}$ and $+Ca^{2+}$, respectively (Lehrer & Morris, 1982), with all three states being inhibitory at low [S1]. Two possibilities exist to explain the apparent discrepancy between these in vitro and structural results. One possibility is that even though S1-induced movement was detected, the probes utilized thus far do not have the correct properties to detect the Ca^{2+}-induced movement of Tm. The other possibility is that the changes in the diffraction pattern interpreted as Tm movement may instead be Ca^{2+}-induced changes in the troponin–actin relationship (Hitchcock, 1975; Potter & Gergely, 1974; Tao et al., 1987; Ishii and Lehrer, preliminary experiments).

ACKNOWLEDGMENTS

We thank Dr. G. Marriott for the lifetime determinations, Dr. E. P. Morris for the curve-fitting cooperative binding computer program, Drs. J. Gergely and P. Graceffa for reading the manuscript, and Prof. G. Weber for helpful comments. The excellent technical assistance of Ms. Nancy Nelson Smith is greatly appreciated.

Registry No. AC, 86636-92-2; L-Cys, 52-90-4.

REFERENCES

Alcala, J. R., Gratton, E., & Prendergast, F. G. (1987) *Biophys. J. 51*, 587–596.

Betteridge, D. R., & Lehrer, S. S. (1983) *J. Mol. Biol. 167*, 481–496.

Bremel, R. D., Murray, J.. M., & Weber, A. (1972) *Cold Spring Harbor Symp. Quant. Biol. 37*, 267–275.

Eaton, B. L. (1976) *Science (Washington, D.C.) 192*, 1337–1339.

Ebashi, S., & Endo, M. (1968) *Prog. Biophys. Mol. Biol. 18*, 123–183.

Eisenberg, E., & Kielley, W. W. (1974) *J. Biol. Chem. 249*, 4742–4748.

Elzinga, M., Collins, J. H., Kuehl, W. M., & Adelstein, R. S. (1973) *Proc. Natl. Acad. Sci. U.S.A. 70*, 2687.

Graceffa, P. (1985) *Biochemistry 24*, 2743–2747.

Graceffa, P., & Lehrer, S. S. (1980) *J. Biol. Chem. 255*, 11296–11300.

Graceffa, P., & Lehrer, S. S. (1984) *Biochemistry 23*, 2606–2612.

Greene, L. (1982) *J. Biol. Chem. 257*, 13993–13999.

Greene, L., & Eisenberg, E. (1980) *Proc. Natl. Acad. Sci. U.S.A. 77*, 2616–2620.

Haselgrove, J. C. (1972) *Cold Spring Harbor Symp. Quant. Biol. 37*, 341–352.

Hill, T. (1983) *Biophys. J. 44*, 383–396.

Hill, T., Eisenberg, E., & Greene, L. (1980) *Proc. Natl. Acad. Sci. U.S.A. 77*, 3186–3190.

Hill, T., Eisenberg, E., & Chalovich, J. M. (1981) *Biophys. J. 35*, 99–112.

Hitchcock, S. E. (1975) *Eur. J. Biochem. 52*, 255–263.

Huxley, H. E. (1972) *Cold Spring Harbor Symp. Quant. Biol. 37*, 361–376.

Hvidt, S. (1986) *Biophys. Chem. 24*, 211–215.

Ishii, Y., & Lehrer, S. S. (1985) *Biochemistry 24*, 6631–6638.

Ishii, Y., & Lehrer, S. S. (1987) *Biochemistry 26*, 4922–4925.

Ishii, Y., & Lehrer, S. S. (1988) *Biophys. J. 53*, 590a.

Johnson, P., & Smillie, L. B. (1975) *Biochem. Biophys. Res. Commun. 64*, 1316-1322.
Kress, M., Huxley, H. E., Faruqi, A. R., & Hendrix, J. (1986) *J. Mol. Biol. 188*, 325-342.
Lamkin, M., Tao, T., & Lehrer, S. S. (1983) *Biochemistry 22*, 3053-3058.
Leavis, P. C., & Gergely, J. (1984) *CRC Crit. Rev. Biochem. 16*, 235-305.
Lehrer, S. S. (1975) *Proc. Natl. Acad. Sci. U.S.A. 72*, 3377-3381.
Lehrer, S. S. (1978) *J. Mol. Biol. 118*, 209-226.
Lehrer, S. S., & Kerwar, G. (1972) *Biochemistry 11*, 1211-1217.
Lehrer, S. S., & Morris, E. P. (1982) *J. Biol. Chem. 257*, 8073-8080.
Macgregor, R. B., & Weber, G. (1986) *Nature (London) 319*, 70-73.
Mak, A., Lewis, W., & Smillie, L. (1979) *FEBS Lett. 105*, 232-234.
Marriott, G. J. (1987) Ph.D. Thesis, University of Illinois.
McLachlan, A. D., & Stewart, M. (1978) *J. Mol. Biol. 103*, 271-298.
Morris, E. P., & Lehrer, S. S. (1984) *Biochemistry 23*, 2214-2220.
Nagashima, H., & Asakura, S. (1982) *J. Mol. Biol. 155*, 409-428.
O'Brien, E. J., Gillis, J. M., & Couch, J. (1975) *J. Mol. Biol. 99*, 461-475.
Okamoto, Y., & Sekine, T. (1985) *J. Biochem. (Tokyo) 98*, 1143-1145.
Phillips, G., Fillers, J. P., & Cohen, C. (1986) *J. Mol. Biol. 192*, 111-131.
Potekhin, S. A., & Privalov, P. L. (1982) *J. Mol. Biol. 159*, 519-535.
Potter, J. D., & Gergely, J. (1974) *Biochemistry 13*, 2697-2703.
Prendergast, F. G., Meyer, M., Carlson, G. L., Iida, S., & Potter, J. D. (1983) *J. Biol. Chem. 258*, 7541-7554.
Ruiz-Opazo, N., & Nadal-Ginard, B. (1987) *J. Biol. Chem. 262*, 4755-4765.
Smillie, L. B. (1979) *Trends Biochem. Sci. (Pers. Ed.) 4*, 151-155.
Stewart, M. (1975) *FEBS Lett. 53*, 5-7.
Tao, T., & Lamkin, M. (1984) *FEBS Lett. 168*, 169.
Tao, T., Lamkin, M., & Lehrer, S. S. (1983) *Biochemistry 22*, 3059-3066.
Tao, T., Gong, B.-J., & Leavis, P. C. (1987) *Biophys. J. 51*, 27a.
Weber, G., & Farris, F. J. (1979) *Biochemistry 18*, 3075-3078.
Weeds, A. G., & Pope, B. (1977) *J. Mol. Biol. 111*, 129-157.
Williams, D. L., & Swenson, C. A. (1981) *Biochemistry 20*, 3856-3864.
Williams, D. L., & Greene, L. E. (1983) *Biochemistry 22*, 2270-2274.
Woods, E. F. (1976) *Aust. J. Biol. Sci. 29*, 405-418.

Multiple Species of Myeloperoxidase Messenger RNAs Produced by Alternative Splicing and Differential Polyadenylation[†,‡]

Kazuya Hashinaka, Chika Nishio, Sook-Jin Hur, Fumio Sakiyama, Susumu Tsunasawa, and Michiyuki Yamada*
Institute for Protein Research, Osaka University, 3-2 Yamadaoka, Suita, Osaka 565, Japan
Received January 20, 1988; Revised Manuscript Received March 24, 1988

ABSTRACT: Three clones of full-length cDNA encoding human myeloperoxidase were isolated from a human leukemia HL-60 cell cDNA library in λgt10 and characterized. Analysis of the nucleotide sequence of one of the cDNA clones, λMP-H17, indicated that the cDNA contained 3207 bp with an open reading frame of 2238 bp, a 5′ noncoding region of 159 bp, a 3′ noncoding region of 800 bp, and a poly(A) tail of 10 bp. cDNA of the two other clones, λMP-H7 and λMP-H14, each contained insertions with shorter sequences of 96 and 82 bp, respectively, on the open reading frame of λMP-H17 cDNA. A myeloperoxidase genomic clone was isolated, and the structure of its 5′ region was determined and compared with the structures of these cDNAs. The comparison revealed that the three cDNAs were derived from myeloperoxidase mRNAs produced by alternative splicing from a transcript of the single gene. Nucleotide sequence analysis of the 3′ region of the cDNAs of several clones indicated that the mRNAs were polyadenylated at five different sites. Amino acid sequence determination of the amino-terminal and carboxy-terminal portions of the myeloperoxidase light and heavy chains revealed that, during processing of a precursor polypeptide into the mature protein, the amino-terminal polypeptide, the small peptide between the light and heavy chains, and the carboxy-terminal amino acid were excised.

Myeloperoxidase is a major hemoprotein present in azurophilic granules of polymorphonuclear leukocytes and is associated with a chloride ion mediated bacteriocidal action of these cells and with modulation of the metabolites generated in response to inflammation (Klebanoff, 1975; Henderson & Klebanoff, 1983). Multiple forms of myeloperoxidase were isolated from human myeloid leukemia HL-60 cells (Yamada et al., 1981) and human leukocytes (Pember et al., 1983; Morita et al., 1986; Miyasaki et al., 1986). The enzymes consisted of two molecules of a 59 000-Da[1] chain and two

[†] This work was partly supported by Grants-in-Aid for Cancer Research from the Ministry of Education, Science and Culture of Japan.
[‡] The nucleic acid sequence in this paper has been submitted to GenBank under Accession Number J02831.
* To whom correspondence should be addressed.

0006-2960/88/0427-5906$01.50/0